Fluoride resistance in Streptococcus mutans

Liao, Ying

Publication date
2017
Document Version
Other version
License
Other

Chapter 4

Common loci related to fluoride resistance in *Streptococcus mutans*

This chapter has been submitted to *Journal of Dental Research* as:
Liao Y, Brandt BW, Yang J, Li J, Crielaard W, van Loveren C, Deng DM.
Genetic loci associated with fluoride resistance in *Streptococcus mutans*.

Abstract

The prolonged exposure of the cariogenic bacterial species *Streptococcus mutans* to high concentrations of fluoride, an anti-caries agent, leads to the development of fluoride resistance in the bacteria. Although fluoride resistance has been considered to be related to chromosomal mutations, very few studies identified genomic regions with relevant mutations. The aim of this study is to identify common loci related to the fluoride resistance in *S. mutans*. By analyzing the available whole genome sequences of two fluoride-resistant *S. mutans* strains and their corresponding wild-type strains, we were able to locate two common chromosomal regions and one common pathway related to fluoride resistance. The corresponding gene expression and enzyme activities were then evaluated. The mutations in *mutp*, the promoter of fluoride antiporter-coding genes, was confirmed to constitutively increase the promoter activity and up-regulate the expression of the downstream fluoride antiporters. Mutations in promoter region *glpFp* resulted in lower expression of *glpF*, coding for glycerol uptake facilitator protein, in fluoride-resistant strains than in wild-type strains. The altered expression of *glpF* implied alterations in membrane permeability, which is related to the influx of fluoride. Mutations were also found in glycolytic enzymes, namely pyruvate kinase and enolase, of fluoride-resistant strains. In one fluoride-resistant strain, *S. mutans* C180-2FR, pyruvate kinase was completely deactivated. In the other fluoride-resistant strain, *S. mutans* UA159FR, enolase was more insensitive to fluoride inhibition than in its wild-type strain. Changes in these glycolytic enzymes may also serve as alternative mechanisms of fluoride resistance. Our results confirmed that common loci are involved in the fluoride resistance of *S. mutans*. These loci are involved in the regulation of fluoride transport and glycolysis. They provide novel candidates for the study of mechanisms of fluoride resistance.

Introduction

Fluoride has been applied for over 50 years as an effective anti-caries agent. The antimicrobial effect of fluoride is a part of its caries-preventive mechanism (Ten Cate 2004). Oral bacteria are known to develop abilities to survive and metabolize in the presence of high levels of fluoride. Fluoride-resistant bacterial strains have been isolated both from clinics and laboratories (Hamilton 1969a; Sheng and Liu 2000; Streckfuss et al. 1980; Van Loveren et al. 1991b). Among them, fluoride-resistant *Streptococcus mutans* strains have been of special interest because of the well-established role of *S. mutans* in cariogenesis (Loesche 1986).

Laboratory-derived fluoride-resistant *S. mutans* strains have been created to understand the mechanism of fluoride resistance (Hoelscher and Hudson 1996; Van Loveren et al. 1989; Zhu et al. 2012). These strains usually possess stable fluoride resistance, which can be maintained more than 50 generations in the absence of fluoride. Recent studies (Liao et al. 2016; Liao et al. 2015; Mitsuhata et al. 2014) revealed that such stable resistance is likely the result of chromosomal mutations. So far, a chromosomal mutation in the promoter region of fluoride antiporter-coding genes has been linked to the acquired fluoride resistance. It was reported that fluoride antiporters can export fluoride ions (F^-) while importing protons (H^+) and hence reduce intracellular fluoride concentration (Baker et al. 2012). The deletion of the fluoride antiporters leads to increased sensitivity of *S. mutans* to fluoride (Men et al. 2016; Murata and Hanada 2016). Previously, we discovered that the fluoride-sensitive *S. mutans* strain UA159 became fluoride resistant when the mutation was introduced in the promoter of the fluoride antiporters. This resistance to fluoride was obtained through up-regulation of the expression of fluoride antiporters (Liao et al. 2016; Liao et al. 2015).

Besides the mutations in the promoter of fluoride antiporter-coding genes, fluoride resistance may be due to other chromosomal alterations. Brussock and Kral isolated fluoride-resistant strains in two steps. The second-step isolates showed stronger resistance than the first-step ones. They thus proposed that multiple genes were involved in fluoride resistance (Brussock and Kral 1987). In the fluoride-resistant strain C180-2FR, we have identified eight single nucleotide polymorphisms (SNPs), including the mutation in the promoter of fluoride antiporters stated above (Liao et al. 2015). These SNPs located either

in the promoter region of functional genes or inside a gene. Although it is unclear whether part or all of the affected genomic regions or proteins play a role in fluoride resistance, the evidence from both studies (Brussock and Kral 1987; Liao et al. 2015) suggested that fluoride resistance may be acquired through mutations in multiple genes, apart or in combination.

Recently, the full genome sequence of another laboratory-derive fluoride resistant strain UA159FR was published in NCBI database (NCBI accession: NZ_CP007016.1). The strain UA159FR was derived from strain UA159, whose genome sequence was already published in 2002 (Ajdic et al. 2002). The available sequence information allows us to compare their genomes and to identify chromosomal mutations. The aim of this study is to investigate common loci with mutations associated with fluoride resistance in *S. mutans*. To this end, we compared the genomes of *S. mutans* UA159 and UA159FR. The mutations found through this comparison were compared with the mutations identified in a previous study, which compared the genomes of *S. mutans* C180-2 and C180-2FR. The gene expression or/and enzyme activities related to the common loci with mutations in both fluoride-resistant strains were further evaluated.

Materials and methods

Bacterial strains and growth conditions

The strains used in this study were *S. mutans* UA159, C180-2 and their derived fluoride-resistant strains UA159FR (kindly provided by Prof. Zhimin Zhang from Jilin University) and C180-2FR (Van Loveren et al. 1989). They were routinely cultured anaerobically (90% N_2, 5% CO_2, 5% H_2) at 37°C using either Brain Heart Infusion (BHI) broth or agar.

Growth of S. mutans UA159FR with fluoride

The ability of *S. mutans* UA159FR to grow with different concentrations of NaF was examined on BHI agar plates. *S. mutans* UA159FR and its parental strain UA159 were characterized with their growth on BHI agar with different levels of sodium fluoride (NaF). Five microliter of 10^1 to 10^5-fold serially diluted overnight cultures were spotted on BHI agar plates supplemented with 0,

2, 4, 6, 12, 25 mM of NaF. All plates were incubated anaerobically at 37°C for 3 d before recording images.

Genome analysis and SIFT prediction

We compared the complete genomic sequences of the wild-type *S. mutans* UA159 (NCBI accession: NC_004350.2) to that of the fluoride-resistant mutant *S. mutans* UA159-FR (NCBI accession: NZ_CP007016.1) to identify SNPs. Firstly, the genomes were aligned using the progressive Mauve method (version 2.4.0, snapshot 2015-02-26) (Darling et al. 2004; Darling et al. 2010). All SNPs provided by Mauve were also manually examined to confirm whether they were located in a coding sequence (CDS) or an intergenic region. For SNPs located in genes, we further checked if the SNP results in an amino-acid change. For SNPs located in intergenic regions, the function of the downstream genes was annotated. The identified SNPs in *S. mutans* UA159FR were compared to those in *S. mutans* C180-2FR (Liao et al. 2015). The scheme for the comparison is shown in Figure 1(A). The common genomic regions with mutations present in the SNP lists of both fluoride-resistant strains were selected for further investigation.

For genes containing mutations in both fluoride-resistant strains, the effect of the consequential amino-acid substitutions on the function of corresponding proteins was predicted with SIFT using the web interface (http://sift.bii.a- star.edu.sg/). Default settings were applied for the prediction (Ng and Henikoff 2003).

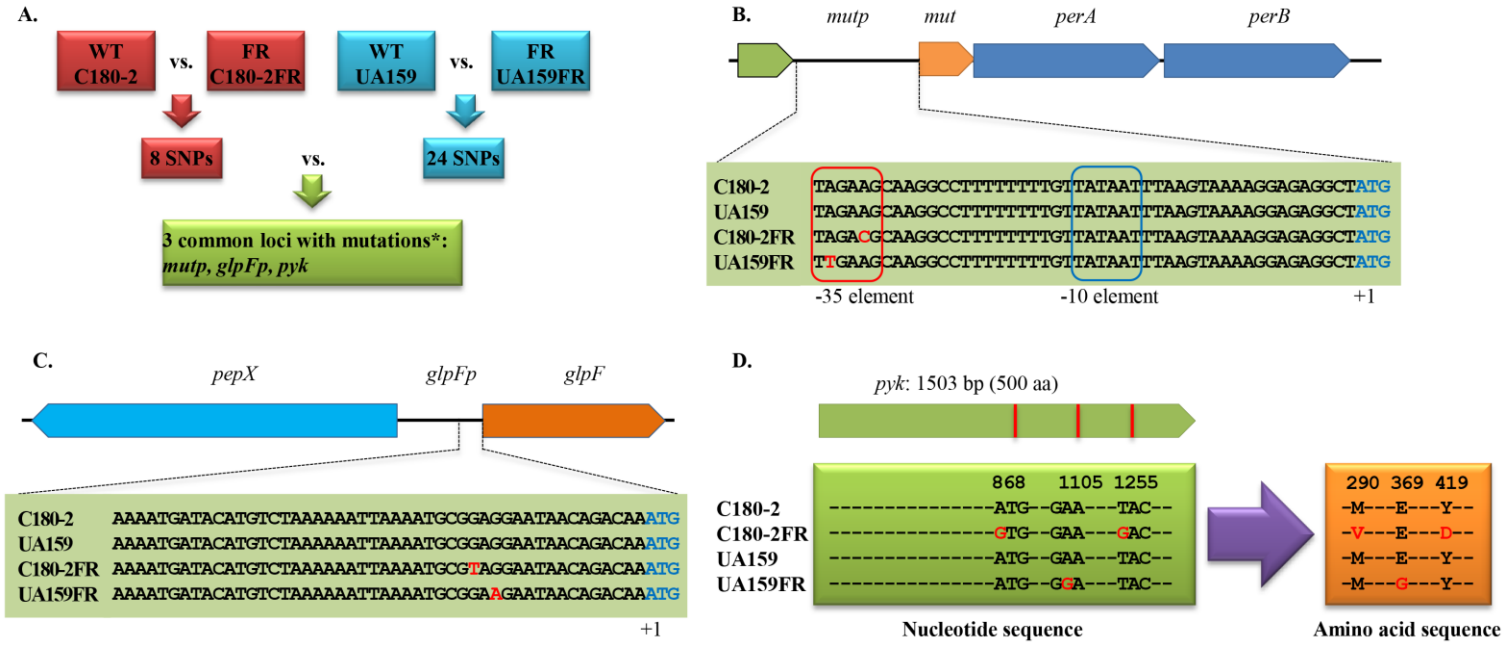

Figure 1. Scheme and results for the identification of common loci with mutations in *S. mutans* UA159FR and C180-2FR. (A) Scheme for the comparison of the SNPs from the two fluoride-resistant *S. mutans* strains. The nucleotide sequence of common loci with mutations in both fluoride-resistant *S. mutans* strains is shown for (B) *mutp*, (C) *glpFp* and (D) *pyk*. WT, wild-type strain; FR, fluoride-resistant strain; SNP, single nucleotide polymorphism; * chromosomal regions in which mutations were found in both fluoride-resistant strains. *perA* and *perB,* encode fluoride antiporters. *glpF,* encodes a glycerol uptake facilitator protein. *pepX,* encodes an x-prolyl-dipeptidyl aminopeptidase. *pyk,* encodes pyruvate kinase. The nucleotides shown in red in (B) to (D) indicate identified SNPs. In (D), the amino acid substitutions due to the SNPs in pyruvate kinase are also shown in red.

Gene expression in S. mutans UA159 and UA159FR

Expression of the genes associated with mutations was examined in *S. mutans* UA159 and UA159FR. Both strains were grown in BHI broth until early exponential phase (OD_{600} = 0.2), late exponential phase (OD_{600} = 0.8) and exponential phase (average OD_{600} = 1.2). Samples were taken from each growth phase and processed as described previously (Liao et al. 2015). Briefly, total RNA was isolated using the Genejet RNA kit (Thermo Scientific, MA, USA), followed by DNase treatment with the TURBO DNA-*free* kit (Life Technologies, Carlsbad, USA) and cDNA synthesis with the RevertAid first strand cDNA synthesis kit (Thermo Scientific, MA, USA). Primers used for tested genes are listed in Supplementary Table 1. *gyrA* and *recA* were used as reference genes (Brenot et al. 2005; Smoot et al. 2001). A $2^{-\Delta\Delta Ct}$ method was used to calculate relative gene expression. The experiment was performed in triplicate.

Construction of green fluorescent protein reporter strains and green fluorescence assay

In order to evaluate the promoter activity alone, the selected promoter regions (*mutp*) obtained from various *S. mutans* strains (UA159, UA159FR, C180-2FR) were separately fused with green fluorescent protein (GFP)-coding gene. Plasmids containing each construct were separately transformed into *S. mutans* strain UA159. The fluorescent intensity of each reporter strain was quantified and compared.

In detail, the *mutp* regions from *S. mutans* UA159, UA159FR and C180-2FR were PCR-amplified with primer *mutp*_gfp_F (5'-3'CATATGAGCCTCTCCTTTTACTTAAA) and *mutp*_gfp_R (5'-3'GCATGCACTGATATTACTGGCTATTTA), and ligated into a shuttle vector pDM45, which contains a promoterless GFP coding gene (*gfpmut2*) (Cormack et al. 1996). As the *mutp* regions from *S. mutans* C180-2 and UA159 are identical, only one wild-type *mutp* reporter construct was made (from UA159). The resulting plasmids were named pLY26 (with the wild-type *mutp*), pLY 27 (with C180-2FR *mutp*) and pLY55 (with UA159FR *mutp*). All constructs were separately transformed into *S. mutans* strain UA159 after the sequences of the insertions were confirmed with Sanger sequencing.

For the green fluorescence assay, overnight cultures of the *S. mutans* reporter strains (*S. mutans* UA159 containing pLY26, pLY27 or pLY55) were

diluted in PBS to approximately 10^7 CFU / ml. After 1 h incubation at 37°C, the fluorescence signals of the dilutions were measured with BD Accuri C6 Cytometer (BD Biosciences, CA, USA) using 488 nm as excitation wavelength and 530 nm as emission wavelength. Ten thousand events were collected in each sample. Data were acquired and analyzed with CFlow software (BD Biosciences, CA, USA). Mean fluorescence intensities (FI) were calculated for events gated from forward-scatter and side-scatter analysis. The corresponding strain containing pDM45 (the construct with promoterless GFP fusion) was used as a negative control. Fluorescence intensities of the reporter strains were calculated by subtracting the mean FI emitted by the negative control from the mean FI of the reporter strains. The experiment was performed in triplicate.

Enzyme activities

Since the glycolytic enzymes were found to be associated with fluoride resistance of both strain UA159FR and C180-2FR (see Results), the activities of pyruvate kinase and enolase were evaluated for both *S. mutans* pairs.

To examine the activity of pyruvate kinase, the late exponential bacterial cells (OD_{600} = 0.8) were harvested with centrifugation at 4,528 x g for 10 min at 4°C, and washed twice with 300 mM HEPES pH 7.0. The cells, resuspended in the same buffer, were challenged with various concentrations (0, 2.5, 5, 10 mM) of NaF in the presence of 0.22 mM glucose. Milli-Q was added to the negative control group. All resuspensions were incubated at 37°C for 30 min. The cells were pelleted with centrifugation at 16,100 x g for 2 min at room temperature. The cell-free extracts were prepared by suspending the pellets with lysis buffer (20 mM Tris-HCl pH 7.5, 0.04% Triton X-100 and complete protease inhibitor) and vigorously beating with 0.1 mm glass beads. The total protein mass of the cell-free extracts was determined with a Bradford protein assay kit (Life Science, Hercules, California, USA) according to the manufacturer's instructions. The cell-free extract was stored at -80°C before used for pyruvate kinase assay (Yamada and Carlsson 1975; Zoraghi et al. 2010). Briefly, pyruvate kinase activity was indirectly determined with two coupled reactions: 1) phosphoenolpyruvate (PEP) + ADP $\rightarrow$ pyruvate + ATP; and 2) pyruvate + NADH + H^+ $\leftrightarrow$ lactate + NAD^+. Pyruvate kinase is responsible for reaction (1) and lactate dehydrogenase is responsible for reaction (2). The reaction mix contained 60 mM Na^+-HEPES pH 7.5, 100 mM KCl, 10 mM $MgCl_2$, 2 mM ADP, 0.24 mM NADH, 0.5 mM glucose-6-phosphate and 12 µg/ml

LDH. Ten mM PEP was added to the experimental group and the same volume of Milli-Q was added to the control group. The reaction was started by adding the 10-fold diluted cell-free extract to the reaction mix and followed by recording absorbance at 340 nm at 25°C for 40 min using the SPECTRAmax PLUS^{384} (Molecular Devices Corp., Sunnyvale, California, USA). The activity of pyruvate kinase was calculated as the amount of pyruvate produced per min per mg total protein. The experiment was repeated four times.

To examine the activity of enolase, permeabilized cells were prepared according to methods described before (Van Loveren et al. 2008). Briefly, cells from mid-exponential phase (OD_{600} = 0.6) were washed with 20 mM potassium phosphate buffer pH 7.0, treated with 10% (v/v) toluene and frozen twice in liquid nitrogen with thawing at 37°C after each freezing. The permeabilized cells were harvested with centrifugation at 4°C at 4000 x g for 5 min and resuspensed in 20 mM potassium phosphate buffer. The enolase activity of these cells was assayed after pre-incubation with 20 mM potassium phosphate buffer pH 7.0 containing 0, 0.5, 1 or 5 mM NaF. The pre-incubation was performed at room temperature (21°C) for 30 min. Then the cells were harvested, washed with Milli-Q and resuspended in enolase assay reaction buffer (20 mM potassium phosphate pH 6.5 with 2 mM $MgSO_4$). Enolase activity was measured as described previously by monitoring the formation of PEP at 240 nm (Van Loveren et al. 2008). Ten microliter of 2-fold diluted permeabilized cells was added to wells of a UV-Star microplate (Greiner Bio-One B.V., Alphen a/d Rijn, the Netherlands) containing 180 µl reaction buffer and 10 µl 2-phosphoglycerate (final concentration 17.6 mM). The assay was followed by recording absorbance at 240 nm at room temperature for 40 min in the SECTRAmax PLUS^{384} (Molecular Devices Corp., Sunnyvale, Calif., USA). The enolase activity was defined as the amount of reduced PEP in the system per min per mg dry weight. The experiment was repeated four times.

Statistics

Data was analyzed with GraphPad Prism (version 5.00, GraphPad Software, San Diego California, USA). Student's *t* test was performed for comparisons for gene expressions between two strains in each growth phase. One-way ANOVA was performed to compare fluorescence intensities of three GFP reporter strains. Two-way ANOVA and following Bonferroni post-tests were performed to compare the activities of enolase and pyruvate kinase under dif-

ferent fluoride concentrations in different strains. p values from the comparisons of gene expressions were corrected for multiple testing using false discovery rate (FDR). Differences were considered statistically significant at $p < 0.05$.

Results

Characterization of growth

In the absence of NaF, *S. mutans* UA159 had a significantly shorter doubling time (54.4 ± 1.7 min) than UA159FR (65.4 ± 0.3 min) in BHI broth. On BHI agar, *S. mutans* UA159FR was able to grow in the presence of higher concentration of fluoride (25 mM) when compared with *S. mutans* UA159 (Figure 2). *S. mutans* C180-2FR, which was characterized in the previous study (Liao et al. 2015), exhibited similar features. It had a significantly longer doubling time than the wild-type strain C180-2 in the absence of NaF, and can also grow in the presence of 25 mM NaF.

Identification of common loci and SIFT prediction for amino acid substitutions

Genome comparison analysis identified a total of 24 SNPs in the genome of *S. mutans* UA159FR (Supplementary Table 2). This list was compared to that from *S. mutans* C180-2FR which was reported previously (Liao et al. 2015). Chromosomal regions containing mutations in both fluoride-resistant strains were identified and shown in Figure 1.

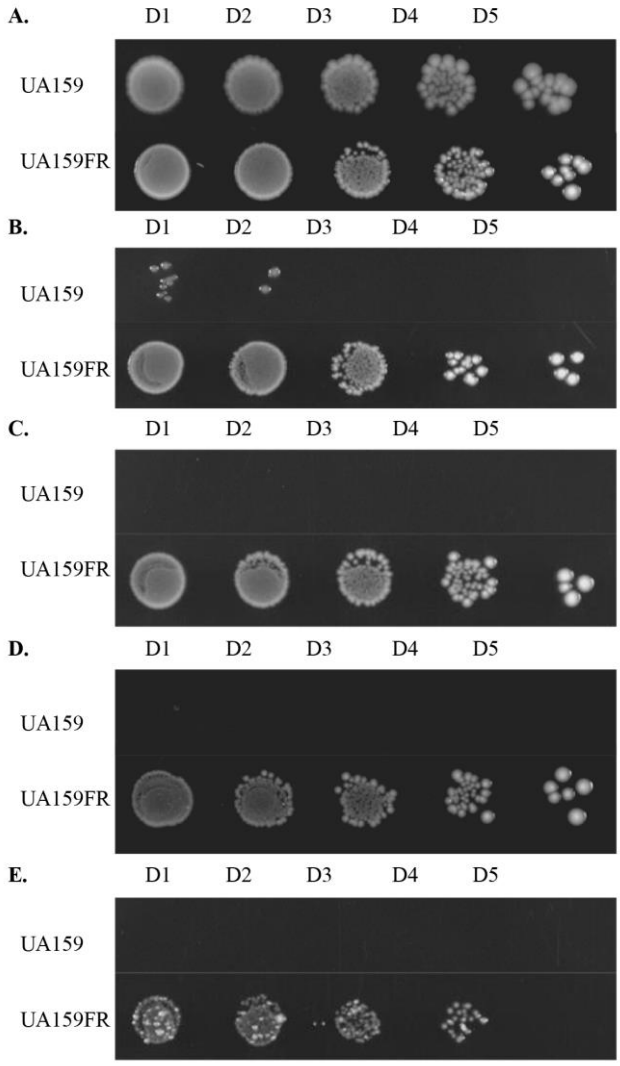

Figure 2. Representative growth of *S. mutans* UA159 and UA159FR on BHI agar plates. NaF is supplemented at increasing concentrations: (A) without NaF; (B) 4 mM NaF; (C) 8 mM NaF; (D) 12 mM NaF; (E) 25 mM NaF. Overnight grown cultures were serially diluted 10^1-fold (D1) to 10^5-fold (D5).

In total, three loci were found to contain mutations in both fluoride-resistant strains. Two of them (*mutp* and *glpFp*) are promoters and one (*pyk*) is a gene from the glycolytic pathway. The nucleotide or amino-acid sequence of these loci are shown in Figure 1(B-D). Mutations found in *mutp* from *S. mutans* C180-2FR and UA159FR were both located in the putative -35 element. Three

downstream genes, encoding a putative mutase (*mut*) and two fluoride antiporters (*perA* and *perB*), are regulated by *mutp* (Figure 1B). The other promoter with mutations, *glpFp,* regulates two genes coding for a glycerol uptake facilitator protein (*glpF*) and an x-prolyl-dipeptidyl aminopeptidase (*pepX*) (Figure 1C). *S. mutans* C180-2FR had two SNPs in *pyk* which led to two amino-acid substitutions (M290V and Y419D), while *S. mutans* UA159FR had one SNP in *pyk* leading to one amino acid substitution (E369G) (Figure 1D). Except the abovementioned loci, a SNP was identified in the enolase-coding gene (*eno*) of *S. mutans* UA159FR (Supplementary Table 2), resulting in one amino-acid substitution (T287I). Enolase catalyzes the reaction upstream of pyruvate kinase, namely the transformation from 2-phosphoglycerate to phosphoenolpyruvate (PEP). As it also plays an important role in glycolysis as pyruvate kinase does, enolase was also examined.

A SIFT prediction was performed for the amino-acid substitutions in pyruvate kinase and enolase. Two of the substitutions in pyruvate kinase, M290V in *S. mutans* C180-2FR and E369G in *S. mutans* UA159FR, were predicted to be tolerated. One substitution in pyruvate kinase of *S. mutans* C180-2FR, Y419D, was predicted to be deleterious to the protein function (score 0.01). The substitution in enolase of *S. mutans* UA159FR (T287I) was predicted to affect protein function (score 0.00) but with low confidence, as the reference sequences were reported to be not diverse enough.

Gene expression and green fluorescence of GFP reporter strains

The expression of seven candidate genes, *mut, perA, perB, glpF, pepX, pyk* and *eno*, was examined for their expression in *S. mutans* UA159 and UA159FR. Mutations were identified either in the coding region or promoter of these selected genes. Figure 3 shows the result of the real-time PCR for samples taken from late exponential phase. All three genes downstream of *mutp*, namely *mut, perA* and *perB*, showed a significantly higher expression in *S. mutans* UA159FR than in UA159. The expression of *mut* in UA159FR was 6-fold higher than in UA159 ($p < 0.0005$), while *perA* and *perB* showed approximately 2-fold up-regulation ($p < 0.05$). One of the downstream genes of *glpFp*, *glpF*, had a significantly lower expression (about 30-fold) in *S. mutans* UA159FR than in UA159 ($p < 0.0005$). The other downstream gene, *pepX*, showed a 3-fold higher expression in UA159FR ($p < 0.005$). The other two tested genes, *pyk* and *eno*, did not show differential expression in *S. mutans* UA159 and UA159FR. The results of samples from early exponential and stationary phases were similar to that from late exponential phase (data not shown). The expression of these genes (except for *eno*) in *S. mutans* C180-2 and C180-2FR were examined in the same manner and reported in our previous study (Liao et al. 2015). Briefly, the expression of *mut, perA* and *perB* in C180-2FR was approximately 10-fold higher than that in C180-2. The expression of *glpF* in C180-2FR was significantly lower than that in C180-2 in early exponential phase. The expression of *pepX* and *pyk* did not differ between *S. mutans* C180-2 and C180-2FR.

The fluorescence intensities (FI) were quantified for three *mutp* GFP reporter strains (Figure 4). Two fluoride-resistant *mutp* reporter strains, *S. mutans* UA159 containing *mutp* from either C180-2FR or UA159FR, showed significantly higher fluorescence (~1450 FI) than the wild-type *mutp* reporter strain (~240 FI) ($p < 0.0005$). No statistically significant difference was found between the FI of the two fluoride-resistant *mutp* reporter strains.

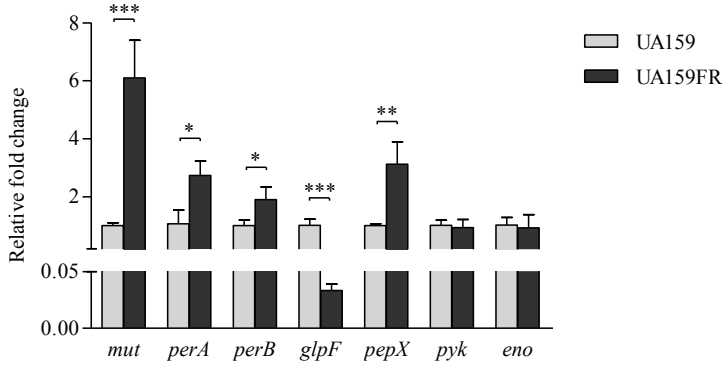

Figure 3. Relative fold change of gene expression between *S. mutans* UA159 and UA159FR. Results from *S. mutans* UA159 and UA159FR at late exponential phase are shown. Overall expression of each selected gene in UA159FR relative to that in UA159 is presented as average fold change ± standard deviation. This experiment was repeated three times. All *p* values were corrected for multiple testing. * $p < 0.05$; ** $p < 0.005$; *** $p < 0.0005$.

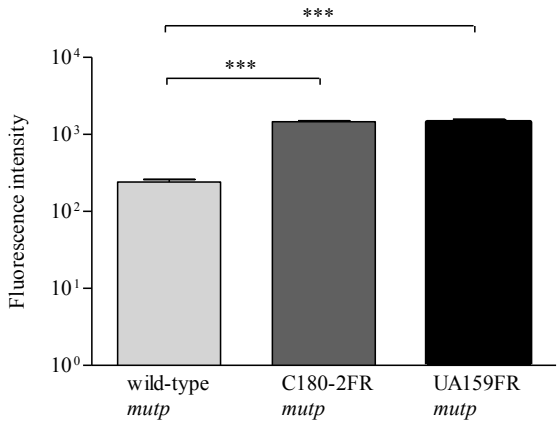

Figure 4. Fluorescence intensities of *mutp* reporter strains, *S. mutans* UA159 containing pLY26 (with the wild-type *mutp*), pLY27 (with the *mutp* from C180-2FR) or pLY55 (with the *mutp* from UA159FR). *** $p < 0.0005$.

Activities of pyruvate kinase and enolase

As we found in our pilot study that pyruvate kinase activity was severely inhibited by excess glucose, we used limited glucose (0.22 mM) in our experiment. The results are shown in Figure 5. *S. mutans* UA159 and its fluoride-resistant derivative UA159FR showed similar pyruvate kinase activities, with all tested concentrations of NaF (Figure 5). *S. mutans* C180-2 and its fluoride-resistant derivative C180-2FR showed completely different activities of pyruvate kinase.

While C180-2 exhibited clearly detectable pyruvate kinase activity under all conditions, C180-2FR displayed no pyruvate kinase activity at all, whether there was NaF present or not (Figure 5).

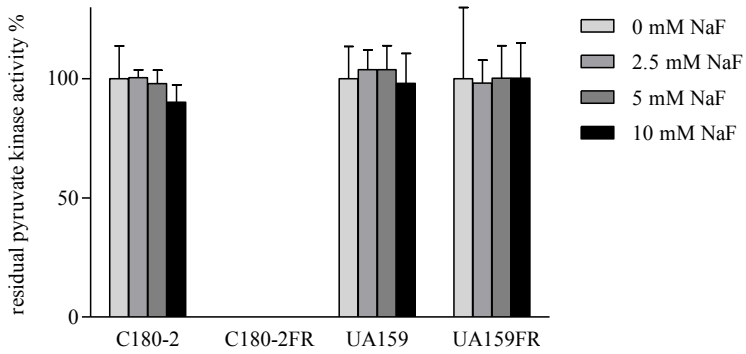

Figure 5. Residual activity of pyruvate kinase in *S. mutans* C180-2, C180-2FR, UA159 and UA159FR after incubation with different concentrations of NaF. The activity of the control group which was incubated without NaF was set at 100%.

Enolase from both *S. mutans* UA159 and UA159FR was inhibited by NaF. The inhibition was stronger in *S. mutans* UA159 than in UA159FR (Figure 6). After pre-incubation with 0.5 mM NaF, only 35% of the original enolase activity remained in *S. mutans* UA159 ($p < 0.001$), while approximately 70% activity was retained in *S. mutans* UA159FR ($p < 0.01$). Increased levels of NaF led to more inhibition in enolase from *S. mutans* UA159, with only 18% residual activity after incubation with 5 mM NaF ($p < 0.001$). For UA159FR, the inhibitory effect of 5 mM NaF is similar to that of 0.5 mM NaF. The enolase activity of *S. mutans* C180-2 and C180-2FR has been evaluated in a previous study (Van Loveren et al. 2008). Enolase from these two strains was similarly inhibited by NaF.

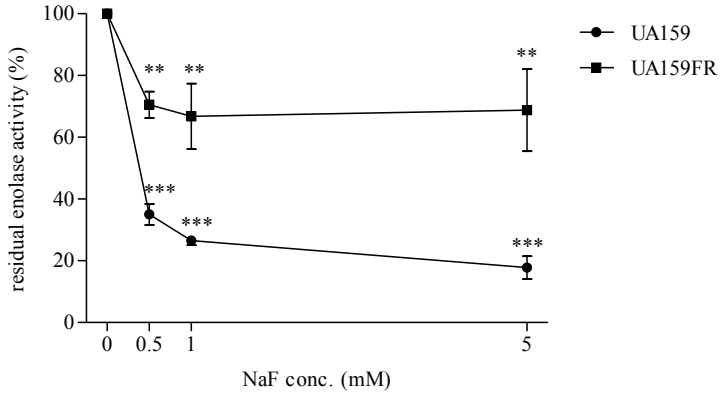

Figure 6. Residual enolase activity of *S. mutans* UA159 and UA159FR after pre-incubation with different concentrations of NaF. The activity of the control group in which no NaF was added during pre-incubation was set at 100%. **, $p < 0.01$; ***, $p < 0.001$.

Discussion

Bacteria can acquire resistance to fluoride through mutation in the promoter of fluoride transporters (Liao et al. 2016). Existing evidence (Brussock and Kral 1987; Liao et al. 2015) indicated that this may not be the only route for a bacterial cell to become fluoride resistant. In this study, we used the available genome sequences of four *S. mutans* strains. By comparing the mutations identified in two fluoride-resistant strains, we were able to locate genes and proteins which are potentially involved in fluoride resistance. We have identified two common chromosomal regions and one common pathway involved in fluoride resistance of *S. mutans*. Our results provide novel candidate loci employed by bacterial cells to acquire fluoride resistance.

In the present study, we found that both fluoride resistant strains *S. mutans* UA159FR and C180-2FR possess mutations in two promoters, *mutp* and *glpFp*. The mutation in *mutp* identified in strain UA159FR further support that regulation of fluoride transporter is likely an important route for bacterial cells to acquire fluoride resistance. However, we noticed different levels of up-regulation in the two fluoride-resistant strains. *S. mutans* UA159FR expressed only 2-3 fold more *perA* and *perB* than its wild-type strain, while *S. mutans* C180-2FR expressed 10-fold more *perA* and *perB* than the wild-type (Figure 3) (Liao et al. 2015). The GFP data failed to explain the difference, as the promoter activities of *mutp* from the two fluoride-resistant strains were similar (Figure

4). We currently do not have an explanation for the difference in fluoride antiporter transcription between the two fluoride-resistant strains.

In contrast to the regulation of fluoride antiporters, the knowledge on the function of mutations in *glpFp* in fluoride resistance is rather limited. Different results were reported for the expression of the downstream gene *pepX* in the *S. mutans* UA159/UA159FR pair and C180-2/C180-2FR pair. The expression of the other downstream gene, *glpF*, was significantly lower in both fluoride-resistant strains than that in the wild-type strains (Figure 3) (Liao et al. 2015). Therefore, we focus on the potential role of *glpF*. This gene encodes a glycerol uptake facilitator protein, which is involved in glycerol metabolism (Ajdic et al. 2002). Very few studies on glycerol metabolism in *S. mutans* are available. However, studies on other species, including *Escherichia coli* and *Lactobacillus sakei*, proposed that a modified glycerol metabolism could lead to changes in membrane properties (Marceau et al. 2004; Truniger and Boos 1993). A *glpF* mutant of *E. coli* had a less permeable membrane than wild-type cells. Interestingly, this mutant was more resistant to a variety of membrane-permeable toxic compounds (Truniger and Boos 1993). Fluoride enters bacterial cells in the form of hydrogen fluoride (HF), which is highly membrane-permeable (Marquis et al. 2003). We believe that the down-regulation of *glpF* leads to decreased membrane permeability and thus serves as an alternative mechanism in bacterial fluoride resistance.

Besides the abovementioned regions, glycolysis is also associated to fluoride resistance. Based on our current data, both *S. mutans* UA159FR and C180-2FR harbor changes in glycolytic enzymes. The involvement of glycolysis, especially the key enzyme enolase, is not surprising. The inhibition of enolase by fluoride is proved to contribute to the antimicrobial action of fluoride (Guha-Chowdhury et al. 1997). This enzyme was proposed to be insensitive to fluoride in fluoride-resistant strains (Bunick and Kashket 1981). However, most previous studies did not find any alteration in either the activity or the gene of enolase (Bunick and Kashket 1981; Van Loveren et al. 2008). In our study, we identified a mutation in the enolase gene of *S. mutans* UA159FR, which results in a profoundly decreased sensitivity of enolase to fluoride inhibition (Figure 6). This enables the bacteria to metabolize in the presence of high levels of fluoride.

In *S. mutans* C180-2FR, instead of enolase, another glycolytic enzyme exhibited different behaviour compared to the wild-type strain. The Y419D substation in pyruvate kinase of C180-2FR resulted in complete deactivation of

this enzyme (Figure 1D and Figure 5). *S. mutans* UA159FR also contained a mutation in pyruvate kinase, however, the mutation did not affect the enzyme function (Figure 1D and Figure 5). Pyruvate kinase catalyzes the transformation from phosphoenolpyruvate (PEP) to pyruvate, which is essential for subsequent acid production (Valentini et al. 2000). Therefore, the malfunction of pyruvate kinase in *S. mutans* C180-2FR can lead to major changes in glycolysis. Alternative pathways may be activated or up-regulated to produce pyruvate. One such pathway can be realized via an aminotransferase (YfbQ), which transfers an amine group from L-alanine to 2-oxoglutarate, with the concomitant production of pyruvate and glutamate (Ajdic et al. 2002; Yoneyama et al. 2011). More studies are needed to confirm the presence of alternative pathways in C180-2FR. The involvement of either enolase or pyruvate kinase indicates that glycolysis is closely related to fluoride resistance. We are currently working on confirming this relationship.

Our current data suggests bacteria can use different approaches to acquire fluoride resistance. A previous study proposed that fluoride resistance is a cumulative effect of multiple genes (Brussock and Kral 1987). We do not know for sure if the identified chromosomal regions contribute synergistically to fluoride resistance. A hint is given by comparing *S. mutans* UA159FR with a genetically engineered strain UF35 (Liao et al. 2016). Unlike UA159FR, which has several common genomic regions with mutations, UF35 only has one mutation in *mutp* which up-regulates the fluoride antiporters. UA159FR is able to grow with much higher level of fluoride than UF35 on BHI agar (Figure 2) (Liao et al. 2016), implying an additive effect of multiple mechanisms. A mutational study is required to directly support the joined effect of the common chromosomal regions.

In conclusion, by comparing the available genomes of fluoride-resistant *S. mutans* strains, we have identified two common chromosomal regions (*mutp* and *glpFp*) and one common pathway (glycolysis) involved in fluoride resistance. Mutations in these loci lead to changes in fluoride transport and glucose metabolism, serving as alternative mechanisms of fluoride resistance in *S. mutans*.

Supplementary information

Supplementary Table 1. qPCR primer sequences and annealing temperatures

Gene name	Primer	Sequence(5'-3')	Product length (bp)	Annealing temperature (°C)
eno	Forward	CGGATATGATGTTCGTGAT	100	57
	Reverse	ACCAAGAATAGCATTAGCA		
glpF	Forward	GTTACCAGATACATTACCA	154	59
	Reverse	TACTGCTCTACTCGTTAT		
mut	Forward	ATGGTGGAGCGATATGTA	146	59
	Reverse	TGTTTAGAAAGACGAATGACT		
perA	Forward	TTACTGCTGCTGGTATGG	131	57
	Reverse	TGCTGATAAGGTTAATACTGTTAG		
perB	Forward	AGATGCTAATCCTTGGTA	140	59
	Reverse	TATGGTCTTCCTCTTCAA		
pepX	Forward	TATGGCTGACTGGACTAA	115	57
	Reverse	TTCCGCAATAATGACCTTA		
pyk	Forward	GGTGAAGATGGCTATTGG	85	59
	Reverse	CATTGGCTCCTTCTGTAAT		

Supplementary Table 2. Single nucleotide polymorphisms identified from the genomes of *S. mutans* UA159 and UA159FR

UA159		UA159FR		Mutation type	Gene annotation
SNP base	Amino acid	SNP base	Amino acid		
G	V	T	F	non_syn[a]	transcriptional regulator (SMU_112c)
T	F	C	S	non_syn	hypothetical protein (SMU_448)
C	S	G	*[b]	non_syn	DNA-directed RNA polymerase subunit omega (rpoZ)
AA	N	CG	R	non_syn	glucosyltransferase-I (gtfB)
C	R	T	C	non_syn	GMP synthase (guaA)
C	T	T	I	non_syn	histidine kinase sensor CiaH (ciaH)
A	E	G	G	non_syn	pyruvate kinase (pyk)
C	T	T	I	non_syn	enolase (eno)
A	*[b]	T	L	non_syn	hypothetical protein (SMU_1292c)
T	S	C	G	non_syn	transposase, ISSmu1 (SMU_565c)
A	S	G	P	non_syn	transposase, IS150-like (SMU_1370c)
G	P	A	L	non_syn	transposase, IS150-like (SMU_1370c)
A		G		intergenic region	Downstream[c]: SMU_t14
C		T		intergenic region	Downstream: SMU_t14
A		G		intergenic region	Downstream: hippurate hydrolase (SMU_318)
G		A		intergenic region	Downstream: hippurate hydrolase (SMU_318)
A		G		intergenic region	Downstream: hippurate hydrolase (SMU_318)
A		G		intergenic region	Downstream: hippurate hydrolase (SMU_318)
G		A		intergenic region	Downstream: glycerol uptake facilitator protein (glpF); x-prolyl-dipeptidyl aminopeptidase (pepX)
C		A		intergenic region	Downstream: Mg2+/citrate transporter (SMU_1013c); hypothetic protein (SMU_1014)
C		A		intergenic region	Upstream[d]: hypothetic proteins (SMU_1546 and SMU_1547c)
C		T		intergenic region	Downstream: transcriptional regulator (SMU_1647c)
C		T		intergenic region	Downstream: SMU_t42

a) nonsyn: non-synonymous coding SNP.
b) *: stop codon.
c) downstream: the gene / genes downstream the intergenic region with the SNP.
d) upstream: the gene / genes upstream the intergenic region with the SNP.